Nanoscale deformations

DOI: 10.1002/smll.200500289

Fluorescent Image Correlation for Nanoscale Deformation Measurements**

*Thomas A. Berfield, Jay K. Patel, Robert G. Shimmin, Paul V. Braun, John Lambros, and Nancy R. Sottos**

Recent advances in nanotechnology have enabled the fabrication of a new generation of materials with highly complex structures. The characteristic length scale of these materials has now outpaced the ability of current techniques to make full-field, nanoscale mechanical property measurements in real time. In addition, biological materials also possess complex structures at the nanoscale, which can affect their resulting larger-scale response. Measurements of bulk properties, while important, offer little information about how the nanostructure influences performance. Localized measurements, such as nanoindentation, provide data that are often difficult to extend to larger length scales. High-resolution imaging techniques such as atomic force or scanning tunneling microscopy (AFM/STM)[1] and near-field scanning optical microscopy (NFSOM),[2] despite being full-field techniques, involve bringing a tip on or very near the surface and thus are not entirely suitable for use with soft (e.g., biological) materials. In addition, these methods require rastering, which limits real-time visualization capability (e.g., of fracture, of the motion and growth of cells, and so on). Fluorescent dyes and particles have enabled a different set of experimental tools for imaging displacements. Fluorescent particles have been widely used in flow visualization and measurement techniques.[3,4] In biological studies, fluorescent dyes indicate the presence of particular microorganisms or track the growth and development of cellular structures.[5–8]

Recent advances in optical techniques have improved discrete fluorescent particle imaging,[9–12] making laboratory nanoscale measurements feasible. Single-particle tracking (SPT) via confocal laser scanning microscopy is a tool used in biophysical research to observe trajectories of small fluorescent particles with nanometer-scale precision.[13,14] Here, we present a powerful full-field technique, fluorescence-based digital image correlation (FDIC), to measure nanoscale deformation in materials using fluorescent nanoparticles. To demonstrate the capabilities of the method, we characterize the complex deformation fields generated around silica microspheres embedded in an elastomer under tensile loading. Displacement resolutions of 20 nm are obtained over a 100×100 μm field of view.

Digital image correlation (DIC) is a data analysis method, which applies a mathematical correlation algorithm to obtain kinematic information from digital images acquired during deformation.[15,16] For conventional two-dimensional (2D) DIC, samples are prepared for testing by the application of a random speckle pattern to their surface. Comparison of successive images reveals a deformed speckle pattern relative to the initial, nondeformed one. The correlation works by matching small square subsets of the nondeformed image (Figure 1a) to locations in the deformed image (Figure 1b). The core of the DIC method lies in the optimization of a correlation coefficient between the two subsets over six parameters characterizing the in-plane deformation; namely the displacements components u and v, and the displacement gradients $\partial u/\partial x$, $\partial u/\partial y$, $\partial v/\partial x$, and $\partial v/\partial y$.[17] The accuracy of the method is approximately ± 0.1 pixels in displacement.

A novel aspect of the current work is that fluorescent nanoparticles are used to create the speckle pattern, enabling the characterization of any material to which the particle pattern can be applied. Fluorescent silica nanoparticles were synthesized and labeled with a rhodamine fluorescent dye (555-nm peak excitation wavelength) according to the procedure outlined by van Blaaderen and Vrij,[18] resulting in a 0.1 % solution (by volume) of nanoparticles in ethanol. The average particle diameter was ≈ 180 nm (Figure 1c). The fluorescent particle solution was spin-cast onto samples of polydimethylsiloxane (PDMS), which had been allowed to fully cure at room temperature. Prior to deposition, all PDMS samples were subjected to a 10-min ultraviolet (UV) surface treatment to enhance particle adhesion. Following deposition and evaporation of the ethanol solution, a single layer of particles remained adhered to the sample surface. The spin-casting rate was varied from 500 to 2500 rpm to produce different pattern densities. The lower spinning rates resulted in patterns with too many agglomerated particles and little dispersion, while the higher spinning rates produced completely uniform patterns with no contrast. A spin-

[*] Prof. N. R. Sottos
Beckman Institute for Advanced Science and Technology
Department of Theoretical and Applied Mechanics
104 S. Wright Street, University of Illinois Urbana-Champaign
Urbana, IL 61801 (USA)
Fax: (+1) 217-244-5707
E-mail: n-sottos@uiuc.edu
T. A. Berfield
Department of Theoretical and Applied Mechanics
University of Illinois Urbana-Champaign, Urbana IL 61801 (USA)
J. K. Patel, Prof. J. Lambros
Department of Aerospace Engineering
University of Illinois Urbana-Champaign, Urbana IL 61801 (USA)
R. G. Shimmin, Prof. P. V. Braun
Frederick Seitz Materials Research Laboratory
Beckman Institute for Advanced Science and Technology
Department of Material Science and Engineering
University of Illinois Urbana-Champaign, Urbana IL 61801 (USA)

[**] N.R.S. and T.A.B. acknowledge the support of AFOSR (MURI Award No. F49550-05-1-0346) and NSF (Award No. CMS-008206). J.L. and J.K.P. would like to acknowledge the support of NSF (Career Grant CMS-9874775) and the UIUC Campus Research Board. P.V.B. and R.G.S. would like to acknowledge the Nanoscale Science and Engineering Initiative of the NSF (Award No. DMR-0117792). R.G.S. acknowledges support from the Fannie and John Hertz Foundation. Some research for this publication was carried out in the Center for Microanalysis of Materials, University of Illinois at Urbana-Champaign, which is partially supported by the U.S. Department of Energy under Award No. DEFG02-91-ER45439.

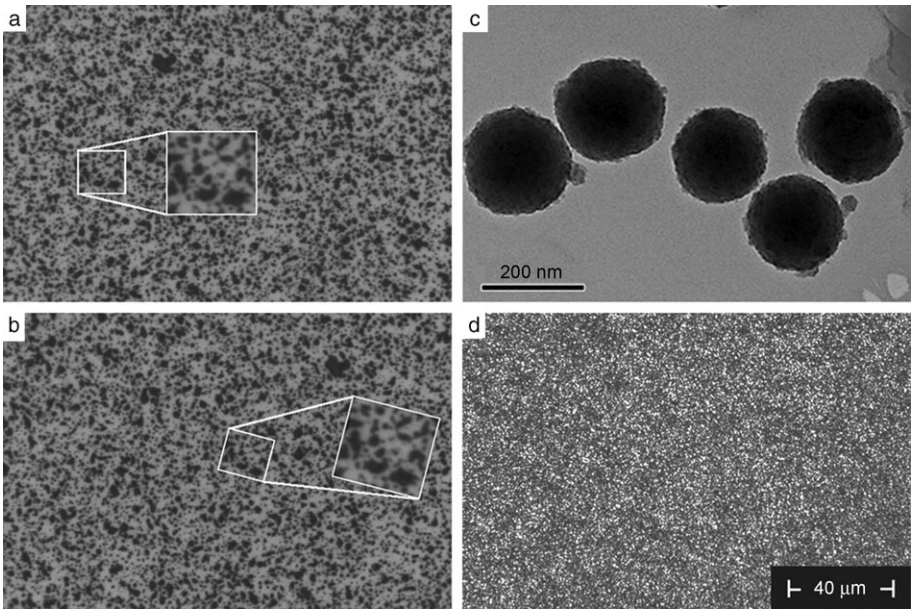

Figure 1. a, b) Representative speckle pattern from previous larger-scale DIC tests[17] before (a) and after (b) applied deformation; c) TEM image of the fluorescent silica nanoparticles; d) fluorescence optical microscope image of fluorescent nanoparticles as deposited on a PDMS sample surface.

ning rate of 1250 rpm produced a monodisperse pattern of particles with an intensity distribution ideal for image correlation analysis (Figure 1 d).

The imaging system consisted of a Leica DM-R fluorescent microscope and a QImaging Retiga monochrome CCD camera with 1280×1024 pixel resolution. The particles were excited by a 542-nm mercury light source and imaged optically. The optical microscope setup, as implemented, provided an optical resolution of 472 nm in transmission and 661 nm in reflection, a maximum displacement resolution of approximately 134 nm per pixel, and overall field of view of 171×137 μm. The resulting fluorescent speckle was approximately 3–4 pixels and a square subset size (S) of 31×31 pixels was used for the correlation.

Photobleaching of the rhodamine dye during the experiment can cause undesirable shifts in pattern intensity, which is unacceptable for correlation between the deformed and nondeformed images. Time-lapse imaging of the particle pattern excited under testing conditions confirmed that significant bleaching did not occur. Similar stability of light intensity was also seen for the rhodamine fluorescent dyes in the work of Ow et al.[19]

The operational limits of the FDIC technique were determined through a series of rigid-body translation and uniaxial tension calibration experiments. For the translation tests, samples were attached to a precision stage driven by a piezoelectric actuator mounted on the microscope platform. Translations ranging from 5 nm to 12 μm were generated by applying a dc voltage to the piezoelectric actuator. Prior to the translation experiments, the piezoelectric actuator was carefully calibrated using a heterodyne interferometer[20,21] over the full range of voltages to produce the desired translation. Images of the sample were acquired before and after translation. The rigid-body displacement field was calculated through numerical correlation of the two images. FDIC measurements were repeated five times for each translation. As shown in Figure 2 a, the FDIC-measured displacements and the applied displacements greater than 100 nm are nearly identical. In the 20–100-nm displacement range, there is more scatter, but the comparison is still excellent (Figure 2 b). Below 20 nm, scatter increases considerably. This scatter is attributed to the stability and accuracy of the piezoactuator response at these low voltage levels, as well as the accuracy of the interpolation scheme for the DIC.

The FDIC technique uses an image intensity interpolation scheme to minimize the correlation coefficient and achieve subpixel displacement accuracy. The limit to which the interpolation scheme can accurately detect subpixel motion during rigid-body translation is illustrated by the measured vector fields in Figure 3. As the size of the applied translation decreases from 50 to 5 nm, nonuniformity of the displacement vectors becomes noticeable below 20 nm and then significant at 5 nm. For translations smaller than 20 nm, the DIC program is unable to accurately measure deformations for this pattern and resolution. The basic noise level of the measurement system (due to ambient vibrations, camera noise, etc.) was ± 2 nm, as determined by correlating successive images at zero displacement. This noise level could be further reduced by frame averaging.[23]

Uniaxial tension tests demonstrate the ability of the technique to detect variations in displacement on the order 20 nm in real time. PDMS samples ($30\ \text{mm} \times 8\ \text{mm} \times 1.2\ \text{mm}$) were loaded under displacement control by a microtensile tester designed for use with the microscope. Control of the actuator and synchronization of the image acquisition with applied displacement was accomplished using Labview (National Instruments). Images were acquired in real time every two seconds for loading rates ranging from $10\ \text{nm s}^{-1}$ to $1\ \mu\text{m s}^{-1}$. FDIC measurements from real-time imaging of the deforming sample were used to calculate the full-field strain and compare its average value to the known applied far-field strain. Typical FDIC-measured contours of displacement in the loading direction are shown in Figure 4 with contributions due to rigid-body translation and rotation removed. The applied far-field displacement recorded at this time instant during loading was 10.7 μm. As expected, displacement increases linearly across the loading direction (x axis) of the sample. The variation of displacement across the field of view is nearly 175 nm with each grayscale level spanning about 10 nm, clearly demonstrating the subpixel accuracy of the DIC technique.[1,2,16] To demonstrate the capability of the FDIC method to measure local strain gradi-

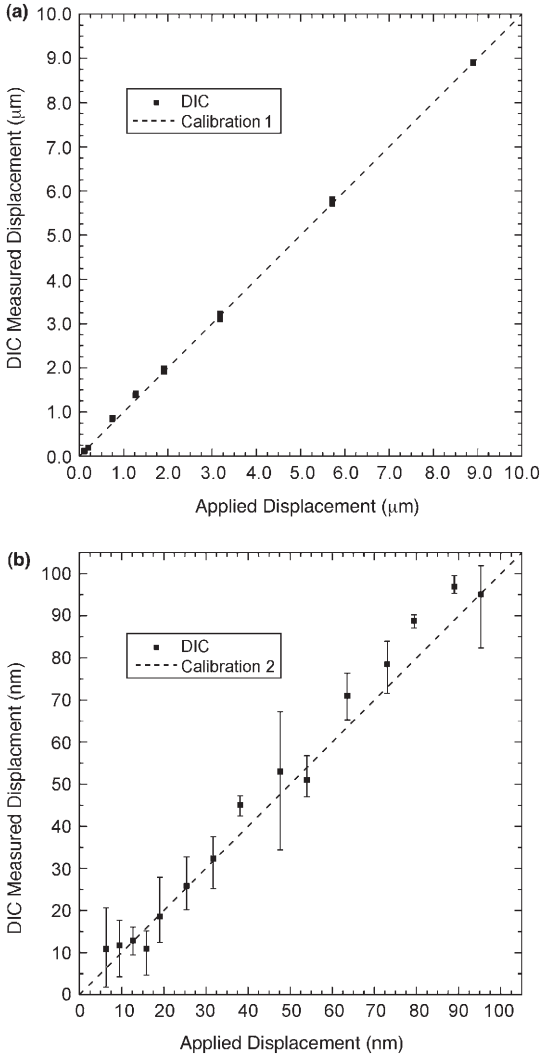

Figure 2. Comparison of DIC results with calibration measurements of rigid-body translations provided by a piezoelectric actuator: a) DIC-measured translations larger than 1 μm are plotted against an optical calibration of the stage; b) average subpixel displacements are compared to a time-averaged dynamic calibration of the piezostack performed with a heterodyne interferometer at 50 Hz.

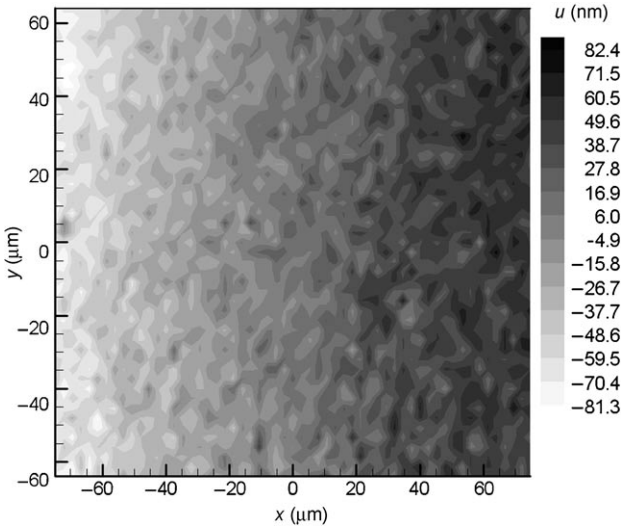

Figure 4. Contour plot of displacements along the *x* direction measured by DIC during a uniaxial tension test. Loading is applied in the horizontal direction (*x* axis) and displacement varies by approximately 170 nm over 140 μm along *x*.

ents, a PDMS sample containing a dilute concentration of silica microspheres (≈40 μm in diameter) was loaded in tension. The mid-plane of the embedded microspheres (Figure 5a) was located 25 μm below the top surface of the sample, which was subsequently spin-coated with fluorescent nanoparticles. A strain concentration is expected in the region surrounding the stiffer inclusions.

Correlating images of the top surface revealed a significant difference in deformation response for the area surrounding the inclusion when compared to the uniform deformation of Figure 4. Contours of constant displacement (shown in Figure 5b) clearly indicate a distortion in the displacement field around a single microsphere. Differentiation of the *u*-direction displacement contours along a line scan through the particle center yielded the localized strain response shown in Figure 5c. Sufficiently far away from the microsphere, the measured strain was nearly constant and

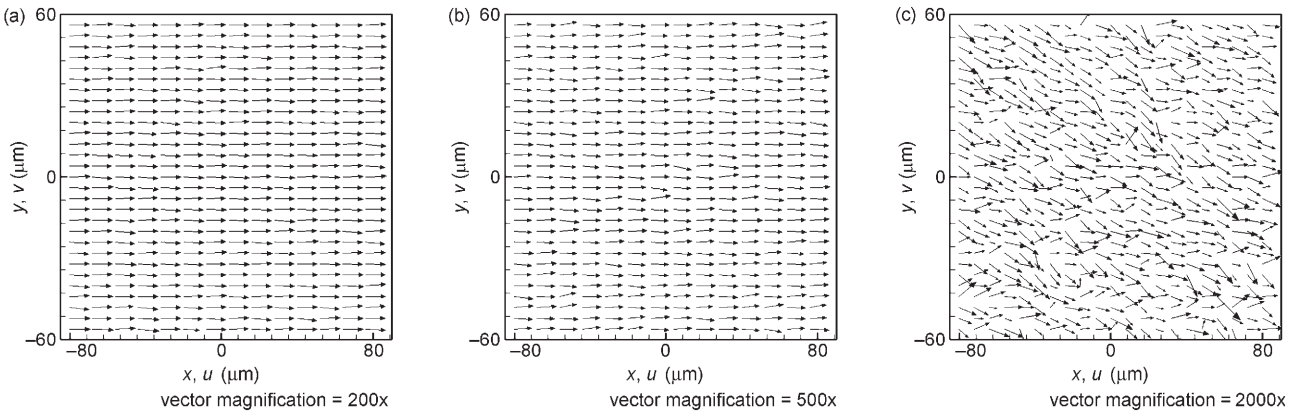

Figure 3. Vector plots of DIC data for a) 50-nm, b) 20-nm, and c) 5-nm applied rigid-body translation. Good correlation is obtained for the 50- and 20-nm images, resulting in uniform displacement values with only a slight scatter. Correlation of the 5-nm applied displacement resulted in large scatter in both *u* and *v* displacements, indicating a practical resolution limit for the current setup between 5 and 20 nm.

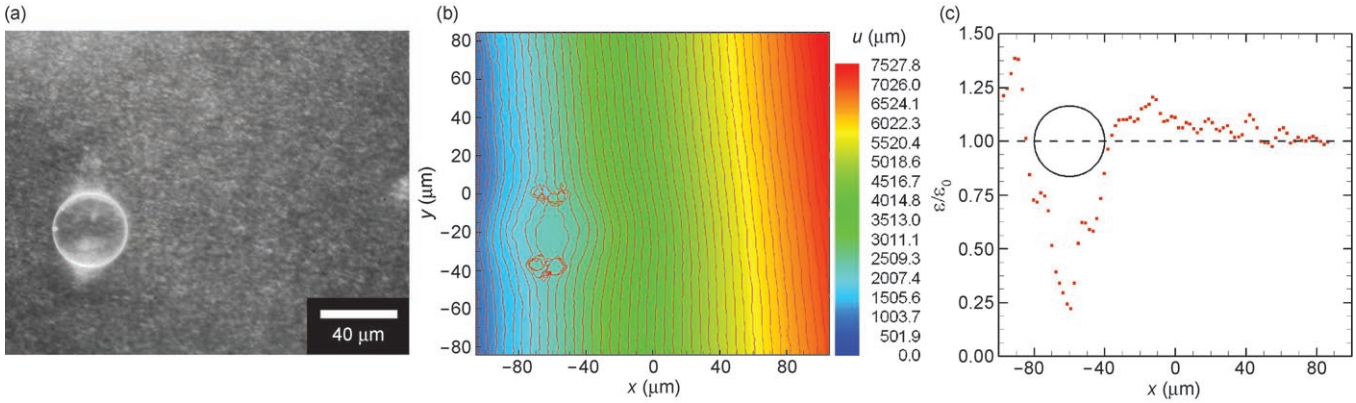

Figure 5. Uniaxial tension test performed on a PDMS sample with a dilute concentration of ≈40-μm silica microspheres: a) single microsphere embedded just below the top surface, b) contours of u displacement for a 3.8% applied strain in the x direction. The irregularities in displacement correlation above and below the inclusion are due to the reflections of the light source from the glass sphere; c) variation in strain in the x direction along a line scan through the center of the microsphere, where ε_0 is the far-field strain.

equal to the globally applied strain, while local to the microsphere a strain concentration was detected.

More complex deformation fields from interactions of multiple inclusions were investigated using an additional sample prepared with a higher concentration of silica microspheres (Figure 6a) and tested in tension. Correlation of the pattern on the top surface indicated regions of low strain response directly above the embedded silica microspheres. Displacement contour plots (Figure 6b) revealed that the high displacement gradients in the PDMS surrounding the inclusions were easily captured by the FDIC method with the same accuracy as displayed in the previous tests.

In summary, FDIC provides a robust methodology for full-field, noncontact, real-time deformation measurements with nanoscale displacement resolution that can be adapted for a wide range of both hard and soft materials. The rigid-body translation calibration experiments established a displacement resolution of 20 nm for the FDIC technique, approximately one-eighth of the size of an image pixel, over a field of view of approximately 100×100 μm. Uniaxial tension testing demonstrated that FDIC can be performed in real time under an optical microscope. Moreover, tension testing of samples with embedded high stiffness inclusions illustrated the ability of FDIC to capture complex deformation fields with high gradients in displacement. Consequently, the applications of FDIC are far reaching since they enable characterization of mechanical performance in material systems with features comparable to the size of the fluorescent nanoparticles, such as ultrathin-film devices, MEMS, and nanocomposites, using a simple optical setup that is noncontact, full-field, real time, yet capable of nanoscale displacement resolution over hundreds of micrometers.

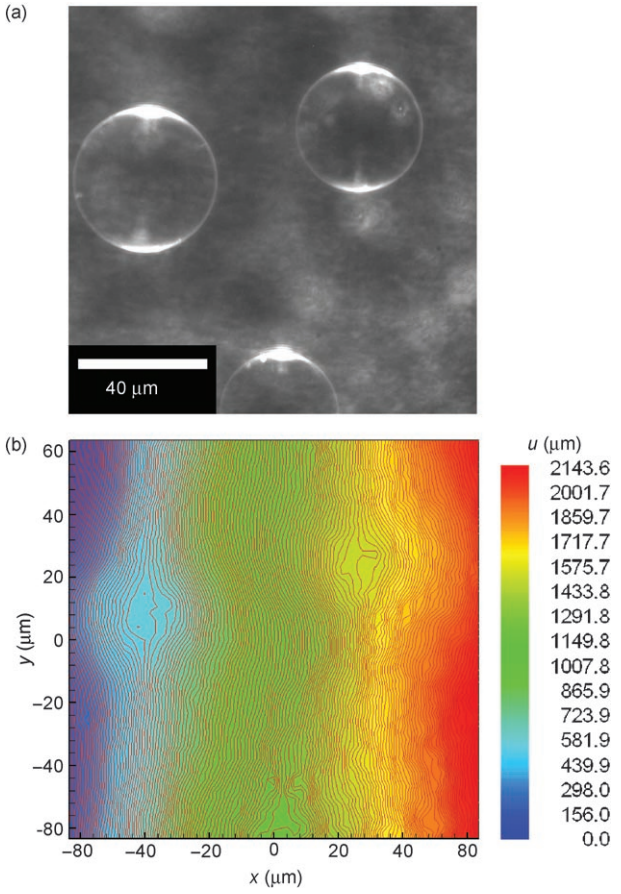

Figure 6. A higher concentration of silica microspheres was used to image a more complex deformation field. a) Three microspheres are imaged 25 μm below the sample surface; b) correlation of the fluorescent particle pattern on the top surface of the PDMS sample generates the displacement field for a uniaxially applied strain of 4.8%.

Keywords:
elastomers · fluorescence · nanomechanics · nanoparticles · silica

[1] G. Vendroux, W. G. Knauss, *Exp. Mech.* **1998**, *38*, 154–160.
[2] I. Chasiotis, W. G. Knauss, *Exp. Mech.* **2002**, *42*, 51–57.
[3] A. Brandt, *Proceedings of the Third International Symposium on Flow Visualization*, **1985**, 279–284.

[4] J. Sakakibara, K. Hishida, M. Maeda, *Int. J. Heat Mass Transfer* **1997**, *40*, 3163 – 3176.
[5] A. P. Synder, D. B. Greenberg, *Biotechnol. Bioeng.* **1984**, *26*, 1395 – 1397.
[6] H. D. A. Lindquist, *Water Res.* **1997**, *31*, 2668 – 2671.
[7] R. Cubeddu, G. Canti, A. Pifferi, P. Taroni, G. Valentini, *Proc. SPIE-Int. Soc. Opt. Eng.* **1997**, *2976*, 98 – 104.
[8] A. Becker, C. Hessenius, K. Licha, B. Ebert, U. Sukowski, W. Semmler, B. Wiedenmann, C. Grötzinger, *Nat. Biotechnol.* **2001**, *19*, 327 – 331.
[9] M. Dahan, S. Levi, C. Luccardini, P. Rostaing, B. Riveau, A. Triller, *Science* **2003**, *302*, 442 – 445.
[10] A. Yildez, J. Forkey, S. McKinney, T. Ha, Y. Goldman, P. Selvin, *Science* **2003**, *300*, 2061 – 2065.
[11] M. Gordon, T. Ha, P. Selvin, *Proc. Natl. Acad. Sci. USA* **2004**, *101*, 6462 – 6465.
[12] O. J. Rolinski, D. J. S. Birch, *J. Chem. Phys.* **2002**, *116*, 10411 – 10418.
[13] A. Gennerich, D. Schild, *Eur. Biophys. J.* **2005**, *34*, 181 – 199.
[14] M. J. Saxton, K. Jacobson, *Annu. Rev. Biophys. Biomol. Struct.* **1997**, *26*, 373 – 399.
[15] W. H. Peters, W. F. Ranson, *Opt. Eng.* **1982**, *21*, 427 – 431.
[16] W. H. Peters, W. F. Ranson, M. A. Sutton, T. C. Chu, J. Anderson, *Opt. Eng.* **1983**, *23*, 738 – 742.
[17] H. A. Bruck, S. R. McNeill, M. A. Sutton, W. H. Peters, *Exp. Mech.* **1989**, *29*, 261 – 267.
[18] A. van Blaaderen, A. Vrij, *Langmuir* **1992**, *8*, 2921 – 2931.
[19] J. L. Abanto-Bueno, J. Lambros, *Exp. Mech.* **2005**, *45*, 144 – 152.
[20] H. Ow, D. R. Larson, M. Srivastava, B. A. Baird, W. W. Webb, U. Wiesner, *Nano Lett.* **2005**, *5*, 113 – 117.
[21] L. Lian, N. R. Sottos, *J. Appl. Phys.* **2000**, *87*, 3941 – 3949.
[22] L. Lian, N. R. Sottos, *J. Appl. Phys.* **1998**, *84*, 5725 – 5728.
[23] B. W. Smith, X. Li, W. Tong, *Exp. Techn.* **1998**, *22*, 19 – 21.

Received: August 16, 2005
Revised: November 20, 2005
Published online on March 15, 2006

